

RSC Advances



This is an *Accepted Manuscript*, which has been through the Royal Society of Chemistry peer review process and has been accepted for publication.

Accepted Manuscripts are published online shortly after acceptance, before technical editing, formatting and proof reading. Using this free service, authors can make their results available to the community, in citable form, before we publish the edited article. This *Accepted Manuscript* will be replaced by the edited, formatted and paginated article as soon as this is available.

You can find more information about *Accepted Manuscripts* in the [Information for Authors](#).

Please note that technical editing may introduce minor changes to the text and/or graphics, which may alter content. The journal's standard [Terms & Conditions](#) and the [Ethical guidelines](#) still apply. In no event shall the Royal Society of Chemistry be held responsible for any errors or omissions in this *Accepted Manuscript* or any consequences arising from the use of any information it contains.



Journal Name

ARTICLE

Preparation, crystal structure and up-conversion luminescence of Er³⁺, Yb³⁺ co-doped Gd₂(WO₄)₃

Received 00th January 20xx,
Accepted 00th January 20xx

DOI: 10.1039/x0xx00000x

www.rsc.org/

Mengyan Yin,^a Yangai Liu,^{a†} Lefu Mei,^{a†} Maxim S. Molokeev,^b Zhaohui Huang,^a and Minghao Fang^a

Up-conversion (UC) phosphors Gd₂(WO₄)₃: Er³⁺/Yb³⁺ were synthesized by a high temperature solid-state reaction method. The crystal structure of Gd₂(WO₄)₃: 3% Er³⁺/10%Yb³⁺ was refined by Rietveld method and it was showed that Er³⁺/Yb³⁺ were successfully doped into the host lattice replacing Gd³⁺. Under 980nm laser excitation, intense green and weak red emissions centered at around 532nm, 553nm, and 669nm were observed, which were assigned to the Er³⁺ ion transitions of ⁴H_{11/2}→⁴I_{15/2}, ⁴S_{3/2}→⁴I_{15/2} and ⁴F_{9/2}→⁴I_{15/2}, respectively. The optimum Er³⁺ doping concentration was determined as 3mol% when the Yb³⁺ concentration was fixed at 10mol%. The pump power study indicated that the energy transfer from Yb³⁺ to Er³⁺ in Er³⁺, Yb³⁺ co-doped Gd₂(WO₄)₃ was a two-photon process, and the related UC mechanism of energy transfer was discussed in detail.

Introduction

Near-Infrared-to-visible (NIR) up-conversion is an optical process, when near infrared photons are converted into visible photons by multiphoton absorption, which is governed with the Anti-Stokes rule.^{1,2} The UC luminescence has attracted a lot of interest from researchers because of its wide potential applications, such as bio-labels, solar cells, optical data storage, displays and so on.³⁻⁹ For UC phosphors, the excellent fluorescence is always achieved by doping rare earth (RE) ions into luminescent hosts. Among various ions, Er³⁺ is the one of the most studied active ions. Since Er³⁺ has a long life of intermediates level and abundant 4f level structure, it can continuously emit green or red photons when excited by high energy photons.¹⁰ In contrast, Yb³⁺ ions are doped as a sensitizer, and it can enhance the near-infrared (around 980nm) absorption and improve the UC luminescent efficiency of Er³⁺.

The host matrixes play a crucial role in the UC process. The good hosts can support doped ions in a fine crystalline field, in which energy transfer (ET) can easily take place in the host, and thus, improve significantly the luminescence properties. To be more specific, host materials should be chemically stable and have low phonon energy to avoid efficiency loss via non-radiative transfer.¹¹ Tungstate crystals are among classic inorganic luminescent materials.¹² In 1896, the X-ray luminescence of CaWO₄ was discovered by Pupin.¹³ The tungstate crystals provide great mechanical strength and chemical and thermal stability.^{14,15} Because of the strong covalent W-O bond in WO₄²⁻ groups, the tungstate can improve the averaged covalency of crystal, and, respectively, the solubility of rare earth ions can be enhanced.¹⁶⁻¹⁹

Of those researches of tungstate doped with rare earth phosphors, most are single tungstate crystals similar to scheelite and double tungstate crystals ALn(WO₄)₂ (A =alkali metal ions, Ln=rare earth ions). While, there is less study on poly-tungstate.

Gadolinium tungstate, Gd₂(WO₄)₃, can be doped easily doped by Er³⁺/Yb³⁺ at Gd³⁺ position because of the similar ionic radius and electrovalence of Gd³⁺ and Er³⁺/Yb³⁺. Besides, the ionic radius of Gd³⁺ is larger than that of Er³⁺ and Yb³⁺, and it can be easily substituted by Er³⁺ and Yb³⁺.^{20,21} Li *et al.*²² prepared Er³⁺/Yb³⁺ co-doped Gd₂(WO₄)₃ via a co-precipitation method, and investigated pumping-route-dependent concentration quenching and temperature effect on the phosphors. Sun *et al.*²³ prepared the Yb³⁺ and Er³⁺ co-doped Gd₂(WO₄)₃ and Gd₂WO₆ using co-precipitation method, and reported the up-converted emission differences between those two phosphors. However, the crystal structure of Gd₂(WO₄)₃ has not been reported, and how the doped ions affect the lattice parameters and structure of Gd₂(WO₄)₃ host has not been discussed.

In this research, Er³⁺/Yb³⁺ co-doped Gd₂(WO₄)₃ phosphors have been synthesized by a conventional high temperature solid-state reaction method. The crystal structure of Gd₂(WO₄)₃: 3% Er³⁺/10%Yb³⁺ is refined by Rietveld method. And the structural characteristics and UC luminescent characteristics of phosphors are investigated. Also, the rare earth ion doping concentration effect on the UC luminescence and the UC mechanism of energy transfer are discussed.

Experimental

The Gd₂(WO₄)₃:xEr³⁺/0.1Yb³⁺ (x=0, 0.001, 0.01, 0.02, 0.03, 0.04, 0.05) phosphors and Gd₂(WO₄)₃:0.03Er³⁺/yYb³⁺ (y=0, 0.05, 0.1, 0.015, 0.2 0.025) phosphors were synthesized by the high temperature solid-state reaction method. The starting materials of Gd₂O₃ (99.99%), Er₂O₃ (99.99%), Yb₂O₃ (99.99%), and WO₃ (A.R.) were mixed based on stoichiometric ratio and ground in an agate mortar. The mixtures were reacted in an aluminum crucible at 1050 °C for 12 hours in resistance furnace in the air. After the

^aSchool of Materials Science and Technology, Beijing Key Laboratory of Materials Utilization of Nonmetallic Minerals and Solid Wastes, National Laboratory of Mineral Materials, China University of Geosciences, Beijing100083, China.

^bLaboratory of Crystal Physics, Kirensky Institute of Physics, SB RAS, Krasnoyarsk 660036, Russia.

† E-mail: liuyang@cugb.edu.cn and mlf@cugb.edu.cn

furnace cooled down naturally, the samples were ground for further test.

The phase composition of as-prepared phosphors was examined by X-ray diffraction measurement (XRD, D8 Advance diffractometer, Bruker, Germany, with Cu-K α and linear VANTEC detector, $\lambda=0.15406\text{nm}$, 40kV, 30mA). The powder diffraction data of $\text{Gd}_2(\text{WO}_4)_3: 3\% \text{Er}^{3+}/10\% \text{Yb}^{3+}$ for Rietveld analysis was collected at room temperature by the step size of $0.02^\circ (2\theta)$, and the counting time was 3 s per step. The Rietveld refinement was performed using package TOPAS 4.2.²⁴ The Fourier transform infrared spectrum (FT-IR) was recorded over the range of $4000\sim 400\text{cm}^{-1}$ by an Excalibur 3100 (USA) device. The diffuse reflection spectra were measured by UV-NIR spectrophotometer (Cary 5000, USA). The UC luminescence spectra were collected at room temperature with a Hitachi F-4600 spectrophotometer equipped with an external power-controllable 980nm semiconductor laser (Beijing Viasho Technology Company, China) as the excitation source.

Results and discussion

The XRD patterns of the as-prepared pure $\text{Gd}_2(\text{WO}_4)_3$, $\text{Gd}_2(\text{WO}_4)_3: \text{Er}^{3+}/\text{Yb}^{3+}$ and the standard PDF diffraction pattern of $\text{Gd}_2(\text{WO}_4)_3$ are shown in Figure 1(a). All the diffraction peaks of the samples fitted well with the standard data of $\text{Gd}_2(\text{WO}_4)_3$ (JCPDS NO. 23-1076), indicating that pure $\text{Gd}_2(\text{WO}_4)_3$ has been successfully synthesized by the high temperature solid-state

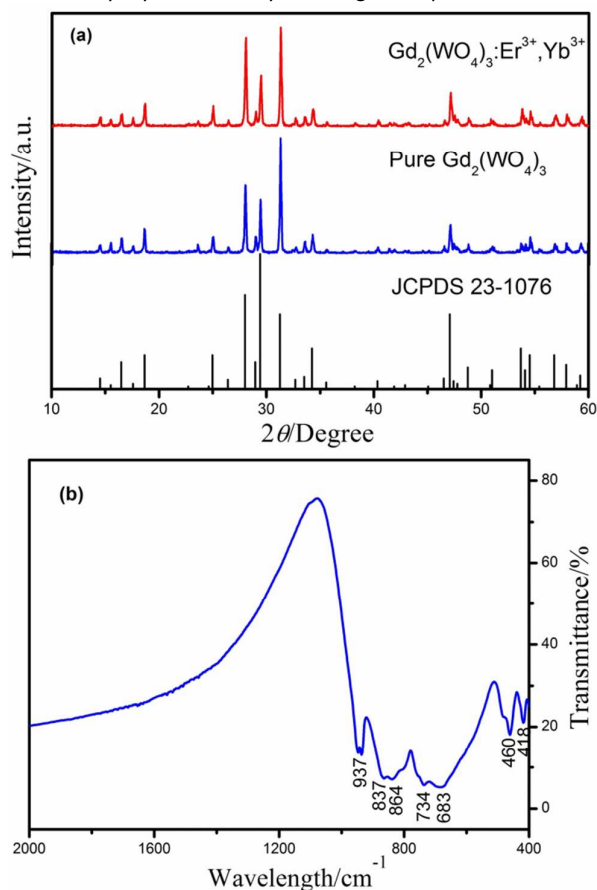


Figure 1 (a) XRD patterns of $\text{Gd}_2(\text{WO}_4)_3$ and $\text{Er}^{3+}/\text{Yb}^{3+}$ co-doped $\text{Gd}_2(\text{WO}_4)_3$ and the standard data of $\text{Gd}_2(\text{WO}_4)_3$ (JCPDS 23-1076) as a reference; (b) FT-IR spectra of pure $\text{Gd}_2(\text{WO}_4)_3$

reaction method at 1050°C for 12h. Besides, the Er^{3+} and Yb^{3+} cannot be detected, which shows that the Er^{3+} and Yb^{3+} are completely doped in the host lattice,²⁵ and did not change the crystal structure of $\text{Gd}_2(\text{WO}_4)_3$.^{26,27} The measurement of the FT-IR spectra of pure $\text{Gd}_2(\text{WO}_4)_3$ is shown in Fig.1 (b). In pure $\text{Gd}_2(\text{WO}_4)_3$, the strong absorption peaks corresponding to the vibrations of WO_4^{2-} groups are between 400 and 1000cm^{-1} . The absorption bands at around 734 and 837cm^{-1} are related to O-W-O stretch vibrations of WO_4^{2-} tetrahedron.^{28,29} The 418 and 460cm^{-1} band can be attributed to the stretching vibration of W-O.³⁰

The structure of $\text{Gd}_2(\text{WO}_4)_3: 3\% \text{Er}^{3+}, 10\% \text{Yb}^{3+}$ is unknown, and, for the Rietveld refinement, the XRD pattern is indexed by monoclinic cell (C2/c) with parameters close to those of $\text{Eu}_2(\text{WO}_4)_3$: (ICSD #15877).^{31,32} The refinement is stable and gives low R-factors (Table 1, Figure 2). The atom coordinates and main bond lengths are listed in Table 2 and Table 3 respectively. The crystal structure of $\text{Gd}_2(\text{WO}_4)_3: 3\% \text{Er}, 10\% \text{Yb}$ is depicted in Figure 3. As seen from Fig.3, the coordination number of Gd^{3+} ions in $\text{Gd}_2(\text{WO}_4)_3$ is eight. The ionic radii of $\text{Gd}^{3+}(\text{CN}=8)=1.053$, while the ionic radii of dopants are $\text{IR}(\text{Yb}^{3+}, \text{CN}=8)=0.985$, $\text{IR}(\text{Er}^{3+}, \text{CN}=8)=1.004$, which are smaller and closer than $\text{IR}(\text{Gd}^{3+}, \text{CN}=8)$.³³ Thus the Gd^{3+} ions are successfully replaced by Yb^{3+} and Er^{3+} ions, which should lead to the host cell parameters shrinkage. The crystallographic data and refinement parameters are shown in Table 1. The cell volume of $\text{Gd}_2(\text{WO}_4)_3: \text{Er}^{3+}, \text{Yb}^{3+}$ is $V=936.65(5)\text{Å}^3$, compared with the stand cell volume of $\text{Gd}_2(\text{WO}_4)_3$, $V=938.15\text{Å}^3$,³⁴ which indicates that the cell volume decrease on the doping by Er^{3+} and Yb^{3+} .

Table 1. Main parameters of processing and refinement of the $\text{Gd}_2(\text{WO}_4)_3: 3\% \text{Er}, 10\% \text{Yb}$ sample

Compound		$\text{Gd}_2(\text{WO}_4)_3: 3\% \text{Er}, 10\% \text{Yb}$	
Sp.Gr.	C2/c	No. of reflections	492
<i>a</i> , Å	7.6541 (2)	No. of refined parameters	66
<i>b</i> , Å	11.4140 (3)	R_{wp} , %	12.66
<i>c</i> , Å	11.3909 (3)	R_p , %	8.67
β , °	109.744(2)	R_{exp} , %	4.83
<i>V</i> , Å ³	936.65 (5)	χ^2	2.62
Z	1	R_B , %	3.35
2θ -interval, °	5-100		

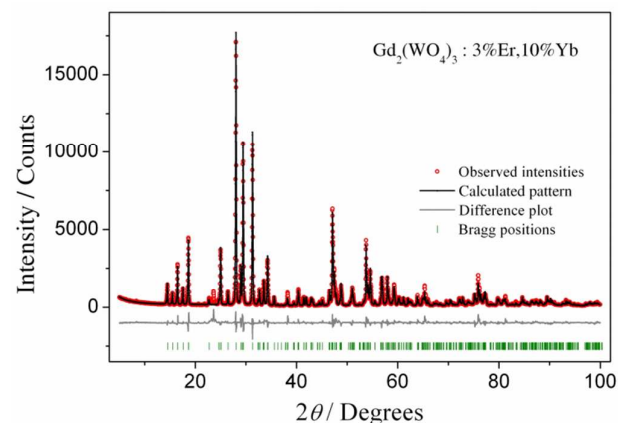


Figure 2 Difference Rietveld plot of $\text{Gd}_2(\text{WO}_4)_3: 3\% \text{Er}, 10\% \text{Yb}$

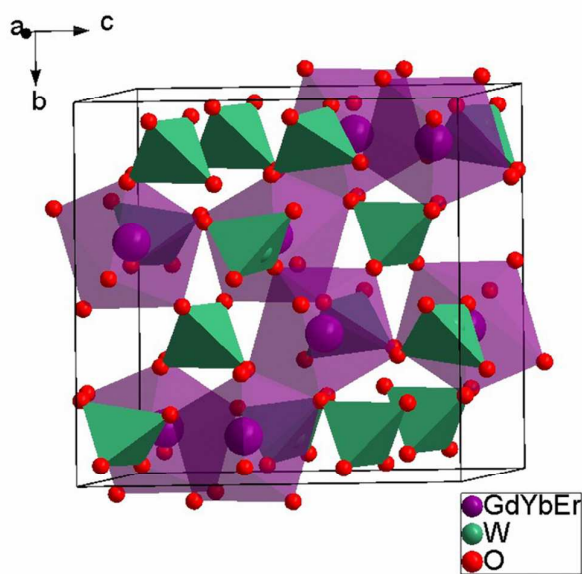
Table 2. Fractional atomic coordinates and isotropic displacement parameters (\AA^2) of $\text{Gd}_2(\text{WO}_4)_3: 3\% \text{Er}, 10\% \text{Yb}$

Atom	x	y	z	B_{iso}	Occ.
Gd	0.3272 (10)	0.3786 (4)	0.4069 (4)	0.3 (3)	0.87
Yb1	0.3272 (10)	0.3786 (4)	0.4069 (4)	0.3 (3)	0.1
Er1	0.3272 (10)	0.3786 (4)	0.4069 (4)	0.3 (3)	0.03
W1	0	0.1327 (3)	0.25	0.6 (3)	1
W2	0.1536 (7)	0.3921 (2)	0.0516 (2)	0.3 (3)	1
O1	0.168 (6)	0.047 (2)	0.223 (4)	1.5 (5)	1
O2	0.126 (6)	0.212 (3)	0.384 (4)	1.5 (5)	1
O3	0.223 (6)	0.324 (3)	0.199 (3)	1.5 (5)	1
O4	0.366 (7)	0.449 (3)	0.040 (3)	1.5 (5)	1
O5	0.060 (7)	0.463 (3)	0.423 (4)	1.5 (5)	1
O6	0.442 (6)	0.210 (3)	0.060 (4)	1.5 (5)	1

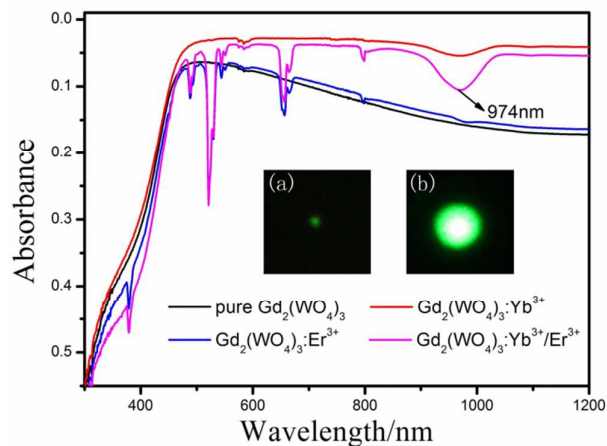
Table 3. Main bond lengths (\AA) of $\text{Gd}_2(\text{WO}_4)_3: 3\% \text{Er}, 10\% \text{Yb}$

(Gd, Yb, Er)—O1 ⁱ	2.43 (3)	W1—O1	1.72 (3)
(Gd, Yb, Er)—O2	2.40 (3)	W1—O2	1.75 (4)
(Gd, Yb, Er)—O2 ⁱⁱ	2.51 (4)	W2—O3	1.76 (3)
(Gd, Yb, Er)—O3	2.31 (4)	W2—O4	1.79 (4)
(Gd, Yb, Er)—O4 ⁱⁱⁱ	2.36 (4)	W2—O5 ^v	1.93 (4)
(Gd, Yb, Er)—O4 ^{iv}	2.44 (3)	W2—O6 ^{vi}	1.70 (4)
(Gd, Yb, Er)—O5	2.33 (4)		
(Gd, Yb, Er)—O6 ⁱⁱⁱ	2.56 (3)		

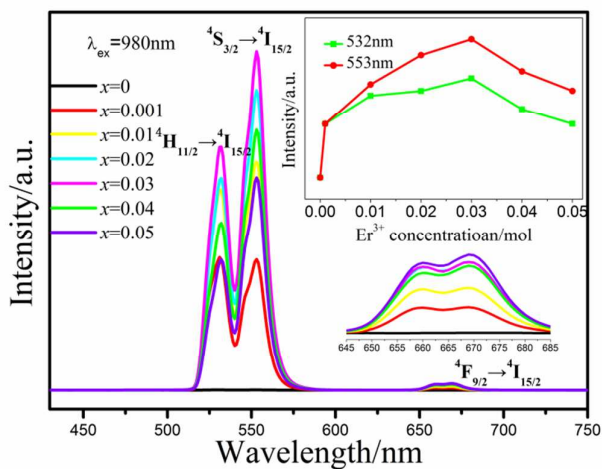
Symmetry codes: (i) $-x+1/2, y+1/2, -z+1/2$; (ii) $-x+1/2, -y+1/2, -z+1$; (iii) $-x+1, y, -z+1/2$; (iv) $x, -y+1, z+1/2$; (v) $-x+1/2, y-1/2, -z+1/2$; (vi) $-x, y, -z+1/2$.

**Figure 3** The crystal structure of $\text{Gd}_2(\text{WO}_4)_3: 3\% \text{Er}, 10\% \text{Yb}$

The diffuse reflection of pure $\text{Gd}_2(\text{WO}_4)_3$, Yb^{3+} doped $\text{Gd}_2(\text{WO}_4)_3$, Er^{3+} doped $\text{Gd}_2(\text{WO}_4)_3$ and $\text{Yb}^{3+}/\text{Er}^{3+}$ co-doped $\text{Gd}_2(\text{WO}_4)_3$ are shown in Fig.4. From the figure, pure $\text{Gd}_2(\text{WO}_4)_3$ does not show apparent absorption in the range of 300~1200nm. The Er^{3+} -doped $\text{Gd}_2(\text{WO}_4)_3$ possesses strong absorption at 520, 655, 795nm, while weak absorption at 974nm is observed. The absorption at 974nm originated from ${}^2F_{7/2} \rightarrow {}^2F_{5/2}$ transition of Yb^{3+} ions is observed in Yb^{3+} -doped $\text{Gd}_2(\text{WO}_4)_3$. Yb^{3+} and Er^{3+} co-doped $\text{Gd}_2(\text{WO}_4)_3$ sample is characterized by the apparent absorption at 520, 655, 795 and 974nm. From the insets, it is obvious that $\text{Yb}^{3+}/\text{Er}^{3+}$ co-doped $\text{Gd}_2(\text{WO}_4)_3$ exhibits higher UC efficiency than that of Er^{3+} -doped $\text{Gd}_2(\text{WO}_4)_3$, which demonstrates that the increasing absorption at 980nm of Er^{3+} is mainly caused by the energy transition of Yb^{3+} to Er^{3+} .

**Figure 4** Diffuse reflection spectra of pure $\text{Gd}_2(\text{WO}_4)_3$, Yb^{3+} doped $\text{Gd}_2(\text{WO}_4)_3$, Er^{3+} doped $\text{Gd}_2(\text{WO}_4)_3$ and $\text{Yb}^{3+}/\text{Er}^{3+}$ co-doped $\text{Gd}_2(\text{WO}_4)_3$, and the inset shows the green luminescence images of the phosphors when irradiated by a 980nm diode (a: Er^{3+} doped $\text{Gd}_2(\text{WO}_4)_3$, b: $\text{Yb}^{3+}/\text{Er}^{3+}$ co-doped $\text{Gd}_2(\text{WO}_4)_3$)

The UC luminescence spectra of single Yb^{3+} doped and $x\text{Er}^{3+}/0.1\text{Yb}^{3+}$ ($x=0-0.05$) co-doped $\text{Gd}_2(\text{WO}_4)_3$ under 980nm near-infrared laser excitation at room temperature is shown in Figure 5, and the inset shows the dependence of green UC emission intensity (at 532nm and 553nm) on Er^{3+} concentration. First of all, Yb^{3+} -doped $\text{Gd}_2(\text{WO}_4)_3$ does not show the UC luminescence because of activator Er^{3+} ions absence. Due to concentration quenching effect,³⁶ UC luminescence green emission intensities

**Figure 5** Comparison of UC luminescence spectra of $\text{Gd}_2(\text{WO}_4)_3: x\text{Er}^{3+}/0.1\text{Yb}^{3+}$ under 980nm laser excitation and the inset shows the intensity of the green emission as a function of Er^{3+} doping concentration and the enlarged red emission band

increase firstly and, then, decrease approaching the maximum at 3mol% of Er^{3+} content (Yb^{3+} concentration was fixed at 10 mol%). In the spectra, two strong green emission bands centered at 532nm and 553nm and a weak red emission band centered at around 669nm are observed, which are assigned to the Er^{3+} ion transitions of $^4\text{H}_{11/2} \rightarrow ^4\text{I}_{15/2}$, $^4\text{S}_{3/2} \rightarrow ^4\text{I}_{15/2}$ and $^4\text{F}_{9/2} \rightarrow ^4\text{I}_{15/2}$, respectively.^{20, 35, 37}

The UC luminescence spectra of single Er^{3+} doped and 0.03 $\text{Er}^{3+}/\text{Yb}^{3+}$ ($y=0-0.25$) co-doped $\text{Gd}_2(\text{WO}_4)_3$ under 980nm near-infrared laser excitation are presented in Figure 6, and the inset shows the variation of the UC luminescent intensity at 532nm and 553nm on the Yb^{3+} concentration increase. Similarly, when singly doped with Er^{3+} ion, the UC spectrum includes very weak UC emission, because Er^{3+} solely can hardly absorb the near-infrared excitation energy in the absence of sensitizer Yb^{3+} ions. With increasing concentration of Yb^{3+} , the UC emission regions are enhanced. Moreover, it is also found that the two strong green emission bands and one weak red emission band are assigned to the Er^{3+} ion transitions.

The UC mechanism can be explained by the dependence of UC emission intensity (I) on pump power (P), which follows the

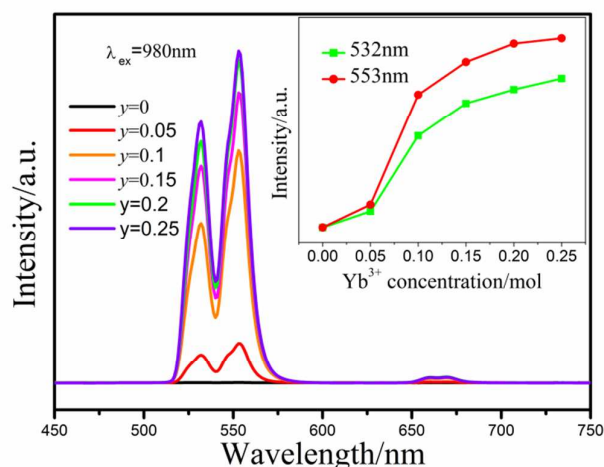


Figure 6 Comparison of UC luminescence spectra of $\text{Gd}_2(\text{WO}_4)_3:0.03\text{Er}^{3+}/y\text{Yb}^{3+}$ under 980nm laser excitation. The inset shows the intensity of the green emission as a function of Yb^{3+} doping concentration

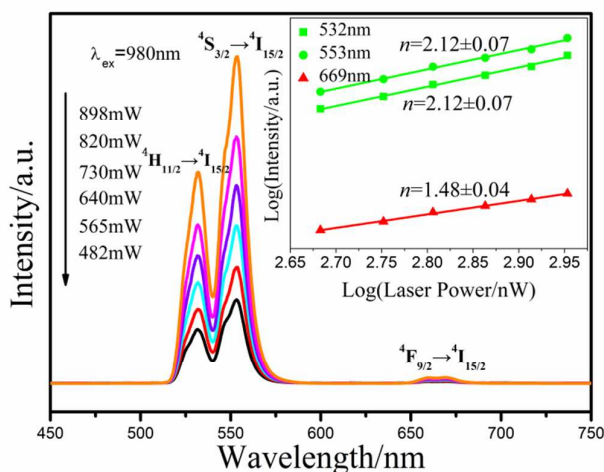


Figure 7 UC emission spectra of $\text{Gd}_2(\text{WO}_4)_3:0.03\text{Er}^{3+}/0.1\text{Yb}^{3+}$ with different pump power, and the inset shows the dependence of green and red UC emission intensities upon pump power.

relation: $I \propto P^n$,^{20, 25, 38} where n is the pump photon number required for the transition from ground state to upper emitting state. The number n is obtained from the slope of the fitting line of $\text{Log } I$ versus $\text{Log } P$. Figure 7 shows the UC luminescence spectrum of $\text{Gd}_2(\text{WO}_4)_3:0.03\text{Er}^{3+}/0.1\text{Yb}^{3+}$ with different pump powers, and the double-logarithmic plot of green and red UC emission intensities upon pump powers is shown in the inset. It is obvious that the UC luminescence intensity of the phosphors increases as the pump power increased. The calculated slopes are 2.12, 2.12 for the green emission (532nm: $^4\text{H}_{11/2} \rightarrow ^4\text{I}_{15/2}$, 553nm: $^4\text{S}_{3/2} \rightarrow ^4\text{I}_{15/2}$), and 1.48 for the red emission (669nm: $^4\text{F}_{9/2} \rightarrow ^4\text{I}_{15/2}$), indicating that both green emission and red emission are two-photon process.^{39, 40, 41}

The deviation from the theoretical value 2 for those special two-photon process may be caused by the crystal structure and the defect states inside the bandgap in the energy transition.^{20, 40} The n value lower than 2 for red emission at 669nm could be due to the large UC rate for the depletion of the intermediate excited states, competition between linear decay, and the local thermal effect as well.²⁵ In the limit of infinitely small UC rates, the UC luminescence intensity for a special n -photon energy transfer tends to be proportional to n -th power of pump power (P^n); while in the limit of infinitely large UC rate, the intensity is proportional to the pump power (P^1). Thus, the UC intensity which excited by the sequential absorption of n photons has a dependence of P^β on pump power, with β ranges from 1 to n .⁴² Besides, as the excitation power is increased, the slope may decrease, which may due to the self-focusing,⁴³ or the high excitation densities may lead to high non-radiative rates and high temperature in the internal samples, and then, the thermal effect causes the quenching of UC intensity.⁴²

According to the above results, the energy level diagram of the Er^{3+} and Yb^{3+} ions and the proposed UC mechanism in $\text{Er}^{3+}/\text{Yb}^{3+}$ co-doped $\text{Gd}_2(\text{WO}_4)_3$ are illustrated in Fig.8. Under the 980nm excitation, Yb^{3+} ion can be excited by one photon and transferred from the ground state $^2\text{F}_{7/2}$ to the excited state $^2\text{F}_{5/2}$. The Er^{3+} ion may be excited and transferred from the ground state $^4\text{I}_{15/2}$ to the excited state $^4\text{I}_{11/2}$ through the ground state absorption (GSA), or may be excited through the energy transfer (ET1) from Yb^{3+} ion. The second step of ET2₁ can promote an excited state absorption (ESA) of Er^{3+} from $^4\text{I}_{11/2}$ to the $^4\text{F}_{7/2}$ level.³⁸

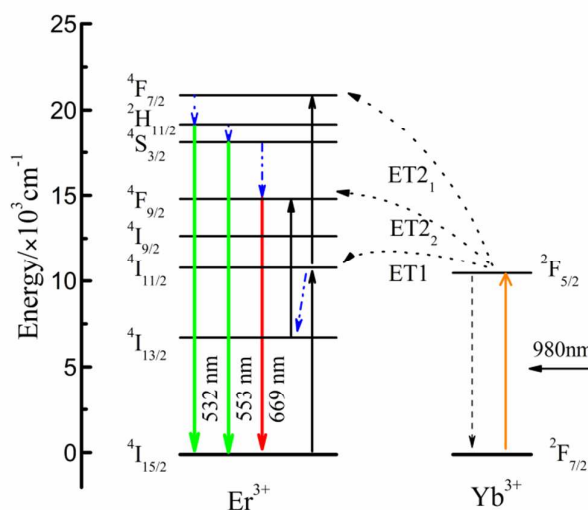


Figure 8 The energy level diagrams of Er^{3+} and Yb^{3+} ions, and the proposed UC mechanism in $\text{Gd}_2(\text{WO}_4)_3:\text{Er}^{3+}/\text{Yb}^{3+}$ phosphors

Because of the small energy gap between the ${}^4F_{7/2}$, ${}^4H_{11/2}$ and ${}^4S_{3/2}$, the transition of Er^{3+} occurred rapidly from the ${}^4F_{7/2}$ to the ${}^4H_{11/2}$ and ${}^4S_{3/2}$ by non-radiative relaxation (NR).³⁵ Finally, the green emissions centered at 532nm and 553nm were produced through radiative transitions of ${}^4H_{11/2} \rightarrow {}^4I_{15/2}$ and ${}^4S_{3/2} \rightarrow {}^4I_{15/2}$. The red emission centered at 669nm was associated with ${}^4F_{9/2} \rightarrow {}^4I_{15/2}$ due to the NR from ${}^4S_{3/2}$ to the ${}^4F_{9/2}$ level or the ET2: ${}^2F_{5/2}(Yb^{3+}) + {}^4I_{13/2}(Er^{3+}) \rightarrow {}^2F_{7/2}(Yb^{3+}) + {}^4F_{9/2}(Er^{3+})$.

Conclusions

Er^{3+} , Yb^{3+} single-doped and Er^{3+}/Yb^{3+} co-doped $Gd_2(WO_4)_3$ phosphors were successfully synthesized by the high temperature solid-state method at 1050°C for 12h. The Er^{3+} and Yb^{3+} doping induced the lattice parameters decrease which proved the Gd^{3+} replacement by Er^{3+} and Yb^{3+} ions. Under the 980nm laser excitation, the Er^{3+} or Yb^{3+} single-doped $Gd_2(WO_4)_3$ samples hardly show the UC luminescence. While the Er^{3+}/Yb^{3+} co-doped $Gd_2(WO_4)_3$ phosphors exhibited remarkable green UC emission at 532 and 553nm and the low-intensity red UC emission at around 669nm, which were assigned to the characteristic level transition of ${}^4H_{11/2} \rightarrow {}^4I_{15/2}$, ${}^4S_{3/2} \rightarrow {}^4I_{15/2}$ and ${}^4F_{9/2} \rightarrow {}^4I_{15/2}$ of Er^{3+} ion, respectively. The optimum Er^{3+} doping concentration was determined as 3mol%. With the Yb^{3+} doping concentration increase, the UC emission intensities of Er^{3+} / Yb^{3+} co-doped $Gd_2(WO_4)_3$ enhanced gradually. The power-dependent luminescent properties indicated that the energy transfer existed in both green and red emissions was a two-photon process. Generally, the results of the present study demonstrates that the Er^{3+}/Yb^{3+} co-doped $Gd_2(WO_4)_3$ is an efficient green emission UC phosphor.

Acknowledgements

The present work was supported by the National Natural Science Foundations of China (Grant No. 51472223), the Fundamental Research Funds for the Central Universities (Grant No. 2652015008), and New Century Excellent Talents in University of Ministry of Education of China (Grant No. NCET-12-0951).

Notes and references

1. F. Auzel, *Chem. Rev.*, 2004, **104**, 139.
2. F. Wang and X. Liu, *Chem Soc Rev*, 2009, **38**, 976-989.
3. L. Shi, C. Li, Q. Shen and Z. Qiu, *Journal of Alloys and Compounds*, 2014, **591**, 105-109.
4. A. Patra, C. S. Friend, R. Kapoor and P. N. Prasad, *Phys. Chem. B*, 2002, **106**, 1909.
5. E. A. Ferreira, F. C. Cassanjes and G. Poirier, *Optical Materials*, 2013, **35**, 1141-1145.
6. K. Teshima, S. Lee, N. Shikine, T. Wakabayashi, K. Yubuta, T. Shishido and S. Oishi, *Crystal Growth & Design*, 2011, **11**, 995-999.
7. A. Shalav, B. S. Richards and M. A. Green, *Solar Energy Materials and Solar Cells*, 2007, **91**, 829-842.
8. X. Li, D. Zhao and F. Zhang, *Theranostics*, 2013, **3**, 292-305.
9. C. Guo, J. Yu, J.-H. Jeong, Z. Ren and J. Bai, *Physica B: Condensed Matter*, 2011, **406**, 916-920.
10. T. Li, C.-F. Guo, Y.-M. Yang, L. Li and N. Zhang, *Acta Materialia*, 2013, **61**, 7481-7487.
11. D. Vennerberg and Z. Lin, *Science of Advanced Materials*, 2011, **3**, 26-40.
12. Q.-H. Zeng, X.-G. Zhang, P. He, H.-B. Liang and M.-L. Gong, *Journal of Inorganic Materials*, 2010, **25**, 1009-1014.
13. G. Blasse, *J. Lumin.*, 1997, **72-74**, 129.
14. V. A. Morozov, A. Bertha, K. W. Meert, S. Van Rompaey, D. Batuk, G. T. Martinez, S. Van Aert, P. F. Smet, M. V. Raskina, D. Poelman, A. M. Abakumov and J. Hadermann, *Chemistry of Materials*, 2013, **25**, 4387-4395.
15. C. Sung Lim, *Journal of Physics and Chemistry of Solids*, 2015, **78**, 65-69.
16. Y. Liu, Y. Y. Jiang, G. X. Liu, J. X. Wang, X. T. Dong and W. S. Yu, *Chinese J. Inorg. Chem.*, 2013, **2**, 277.
17. S. Han, B. Song, L. Liu, C. He and K. S. Yang, *Chin. J. Lumin.*, 2013, **9**, 1183.
18. Y. Lin, S. K. Gao, G. M. Wang and W. M. Shi, *J. Fuzhou Univ.*, 2008, **1**, 134.
19. V. V. Atuchin, E. N. Galashov, O. Y. Khyzhun, A. S. Kozhukhov, L. D. Pokrovsky and V. N. Shlegel, *Crystal Growth & Design*, 2011, **11**, 2479-2484.
20. Z. Xia, J. Li, Y. Luo, L. Liao and J. Varela, *Journal of the American Ceramic Society*, 2012, **95**, 3229-3234.
21. K. R. Kort and S. Banerjee, *Inorg Chem*, 2011, **50**, 5539-5544.
22. J. Li, J. Sun, J. Liu, X. Li, J. Zhang, Y. Tian, S. Fu, L. Cheng, H. Zhong, H. Xia and B. Chen, *Materials Research Bulletin*, 2013, **48**, 2159-2165.
23. M. Sun, L. Ma, B. J. Chen, F. Steponzgi, F. Liu, Z. W. Pan, M. K. Lei and X. J. Wang, *Journal of Luminescence*, 2014, **152**, 218-221.
24. Bruker AXS TOPAS V4 – User's Manual. Bruker AXS, Karlsruhe, Germany. 2008.
25. M. Pollnau, D. R. Gamelin, S. R. Luthi and H. U. Gudel, *Phys. Rev. B.*, 2000, **61**, 3337.
26. J. Chen, Y.-g. Liu, H. Liu, D. Yang, H. Ding, M. Fang and Z. Huang, *RSC Advances*, 2014, **4**, 18234.
27. C. Guo, Y. Xu, X. Ding, M. Li, J. Yu, Z. Ren and J. Bai, *Journal of Alloys and Compounds*, 2011, **509**, L38-L41.
28. A. Durairajan, D. Thangaraju, D. Balaji and S. Moorthy Babu, *Optical Materials*, 2013, **35**, 740-743.
29. X. Yu, M. Gao, J. Li, L. Duan, N. Cao, Z. Jiang, A. Hao, P. Zhao and J. Fan, *Journal of Luminescence*, 2014, **154**, 111-115.
30. F. Lei and B. Yan, *Journal of Solid State Chemistry*, 2008, **181**, 855-862.
31. D. H. Templeton and A. Zalkin, *Acta. Cryst.*, 1963, **16**, 762.
32. V. V. Atuchin, A. S. Aleksandrovsky, O. D. Chimitova, T. A. GavriloVA, A. S. Krylov, M. S. Molokeev, A. S. Oreshonkov, B. G. Bazarov and J. G. Bazarova, *The*

ARTICLE

Journal Name

- Journal of Physical Chemistry C*, 2014, **118**, 15404-15411.
33. R. D. Shannon, *Acta Cryst.*, 1976, **A32**, 751.
34. K. Nassau, H. J. Levinstein and G. M. Loiacono, *J. Phys. Chem. Solids.*, 1965, **26**, 1805.
35. M. Guan, H. Zheng, L. Mei, M. S. Molokeev, J. Xie, T. Yang, X. Wu, S. Huang, Z. Huang and A. Setlur, *Journal of the American Ceramic Society*, 2015, **98**, 1182-1187.
36. M. Y. Peng, N. Zhang, L. Wondraczek, J. R. Qiu, Z. M. Yang and Q. Y. Zhang, *Opt. Express*, 2011, **19**, 20799.
37. Y. Wang and J. Ohwaki, *Applied Physics Letters*, 1993, **63**, 3268.
38. P. Du, Z. Xia and L. Liao, *Journal of Luminescence*, 2013, **133**, 226-229.
39. D. Dai, S. Xu, S. Shi, M. Xie and C. Che, *Optics letters*, 2005, **30**, 3377-3379.
40. J. Zhang, Y. Wang, L. Guo and P. Dong, *Dalton Transactions*, 2013, **42**, 3542-3551.
41. L. Xing, Y. Xu, R. Wang, W. Xu, S. Gu and X. Wu, *Chemical Physics Letters*, 2013, **577**, 53-57.
42. J. Zhang, Y. Wang, L. Guo, F. Zhang, Y. Wen, B. Liu and Y. Huang, *Journal of Solid State Chemistry*, 2011, **184**, 2178-2183.
43. H. Yang, S. Xu, C.-H. Tao, V. W.-W. Yam and J. Zhang, *Journal of applied physics*, 2011, **110**, 043105.

Preparation, crystal structure and up-conversion luminescence of

Er³⁺, Yb³⁺ co-doped Gd₂(WO₄)₃

Mengyan Yin,^a Yangai Liu,^{a†} Lefu Mei,^{a†} Maxim S. Molokeev,^b Zhaohui Huang,^a and Minghao Fang^a

^a School of Materials Science and Technology, Beijing Key Laboratory of Materials Utilization of Nonmetallic Minerals and Solid Wastes, National Laboratory of Mineral Materials, China University of Geosciences, Beijing100083, China.

^b Laboratory of Crystal Physics, Kirensky Institute of Physics, SB RAS, Krasnoyarsk 660036, Russia.

† E-mail: liuyang@cugb.edu.cn and mlf@cugb.edu.cn

Graphical abstract

The crystal structure of Er³⁺ and Yb³⁺ co-doped Gd₂(WO₄)₃ and the brilliant up-conversion green emission.

